

Published in final edited form as:

NMR Biomed. 2008 July ; 21(6): 589–597. doi:10.1002/nbm.1229.

Axonal injury detected by *in vivo* DTI correlates with neurological disability in a mouse model of Multiple Sclerosis

Matthew D. Budde, BS¹, Joong Hee Kim, PhD¹, Hsiao-Fang Liang, MS¹, John H. Russell, PhD², Anne H. Cross, MD³, and Sheng-Kwei Song, PhD^{1,*}

¹Department of Radiology, Washington University, 660 S. Euclid Avenue, St. Louis, MO, 63110, USA

²Department of Molecular Biology and Pharmacology, Washington University, 660 S. Euclid Avenue, St. Louis, MO, 63110, USA

³Department of Neurology and Neurosurgery, Washington University, 660 S. Euclid Avenue, St. Louis, MO, 63110, USA

Abstract

Recent studies have suggested that axonal damage, and not demyelination, is the primary cause of long-term neurological impairment in Multiple Sclerosis (MS) and its animal model, experimental autoimmune encephalomyelitis (EAE). The axial and radial diffusivities derived from diffusion tensor imaging (DTI) have shown promise as noninvasive surrogate markers of axonal damage, and demyelination, respectively. In the current study, *in vivo* DTI of the spinal cords from mice with chronic EAE was performed to determine if axial diffusivity correlated with neurological disability in EAE assessed by the commonly used clinical scoring system. Axial diffusivity in the ventrolateral white matter had a significant negative correlation with EAE clinical score and was significantly lower in mice with severe EAE than mice with moderate EAE. Furthermore, the greater decreases in axial diffusivity were associated with greater amounts of axonal damage as confirmed by quantitative staining for non-phosphorylated neurofilaments (SMI-32). Radial diffusivity and relative anisotropy could not distinguish between the groups of mice with moderate EAE and those with severe EAE. The results further the notion that axial diffusivity is a noninvasive marker of axonal damage in white matter and could provide the necessary link between pathology and neurological disability.

Keywords

Diffusion tensor imaging; axial diffusivity; radial diffusivity; spinal cord; experimental autoimmune encephalomyelitis; axonal damage; demyelination; white matter

Introduction

Magnetic resonance imaging (MRI) has become an indispensable tool for the diagnosis and management of patients with multiple sclerosis (MS). The identification of lesions on T2-weighted images is part of the criteria for the diagnosis of MS (1). In this regard, MRI has revolutionized the diagnosis of MS. However, the relationship between brain abnormalities identified with MRI and clinical impairment has not been as straightforward, and has led to

*Send correspondence to: Sheng-Kwei "Victor" Song, Ph.D., Biomedical MR Laboratory, Campus Box 8227, Washington University, School of Medicine, 660 S. Euclid Avenue, St. Louis, MO 63110, USA, Phone: (314) 362-9988, Fax: (314) 362-0526, Email: ssong@wustl.edu

the clinical-radiological paradox in MS. The MRI measures that have been used for diagnosis, including T2-lesion load and number of contrast-enhanced T1-weighted lesions, have had only modest correlations with clinical impairment. Because of the poor correlations, the use of MRI as a surrogate outcome measure in clinical trials has come under intense scrutiny by both the U.S. Food and Drug Administration and clinical researchers (2-4). A number of different pathological processes (inflammation, demyelination, and axonal damage) may result in abnormalities on conventional T1- and T2-weighted images. Recent work has advanced the idea that axonal damage is a major component of MS and believed to be the cause of long-term clinical impairment. However, conventional MR measures have been unable to provide a link between pathology and clinical disability.

Diffusion tensor imaging (DTI) has shown promise as a non-invasive marker of specific pathology. DTI measures the diffusion of water molecules, which reflect the microstructural organization of the tissues of interest. The white matter of the central nervous system is highly ordered and has a coherent structure in which water diffusion parallel to the fibers, axial diffusivity (λ_{\parallel}), is much greater than the diffusion of water perpendicular to the fibers, radial diffusivity (λ_{\perp}). These directional diffusivities derived from DTI have been shown to reflect changes in white matter pathology in several animal models (5-7). Specifically, demyelination is associated with an increase in radial diffusivity, presumably due to the loss of myelin membrane integrity that hinders water diffusion perpendicular to their orientation (8). In contrast, axonal damage is associated with a decrease in axial diffusivity. Although the underlying mechanism is still unclear, the decreased axial diffusivity could result from the loss of coherent organization of the axon (9) and many other structural and physiologic mechanisms associated with axon damage and degeneration (6). Although measures of anisotropy derived from DTI are commonly used as biomarkers of white matter pathology, an increase in radial diffusivity or a decrease in axial diffusivity will both cause a decrease in anisotropy. Therefore, while anisotropy is an exquisitely sensitive marker of pathology, it is not specific to either axonal damage or demyelination. The available evidence suggests that axial and radial diffusivities hold promise as specific biomarkers of white matter pathology.

It is hypothesized that the directional diffusivities derived from DTI, specifically those reflecting axonal damage, could establish a link between imaging and neurological disability that has escaped conventional MRI measures. The purpose of the current study is to use *in vivo* DTI of the spinal cord of mice with experimental autoimmune encephalomyelitis (EAE), a mouse model of MS, to determine if axial diffusivity, a marker of axonal damage, or radial diffusivity, a marker of demyelination, correlate with the degree of neurological disability and histological measures of axonal damage and demyelination.

Materials and Methods

Animals

All animal procedures were approved by the Washington University Animal Studies Committee and conformed to the Policy on Animal Care. Two groups of 6-8 week old C57BL/6 mice (Jackson Labs, Bar Harbor, ME) were employed in the present study. A cohort of six male mice underwent adoptive transfer of $\sim 2 \times 10^6$ CD4 Thy1.1 MOG-activated T-cells as previously described (10) for EAE induction. The second group of 10 female mice underwent active immunization with 50ug MOG₃₅₋₅₅ emulsified in incomplete Freund's adjuvant with 50ug mycobacterium tuberculosis for EAE induction. A cohort of five female mice served as controls. The selection of gender was arbitrary, and there are no known gender differences for MOG-induced EAE mice (11). Mice were evaluated daily using a published 0-5 clinical scoring system: 1 = limp tail; 2 = hind limb weakness sufficient to impair righting; 3 = one limb paralyzed; 4 = two limbs paralyzed; 5 = more than 2 limbs paralyzed or the animal is moribund (12).

Diffusion Tensor Imaging

Mice with adoptively transferred EAE underwent imaging following the induction of the disease at six time points selected according to the appearance of clinical signs. Mice were imaged at baseline (day 0), before the onset of clinical impairment (~days 3 and 6), the day of onset of clinical signs (~day 8), at the end of the acute period when recovery was commencing (~day 16), and in the chronic stable phase (~day 26). The group of mice with EAE induced by active immunization underwent imaging in the chronic phase of the disease (~day 25). These mice had maintained a stable EAE score that did not deviate by more than 1 in the 10 days prior to being imaged. Control mice were imaged at corresponding ages.

Mice were anesthetized using 5% isoflurane in oxygen, fitted with a custom nose cone to deliver 1% isoflurane in oxygen for maintenance, and placed in a custom holder designed to isolate spinal cord motion (13). A 9-cm i.d. Helmholtz coil was employed as the RF transmitter. The receiver coil consisted of an inductively-coupled surface coil constructed with a 9×16 mm i.d. tailored to fit comfortably around the spine of the mouse (13). The entire preparation was placed in an Oxford Instruments 200/330 magnet (4.7 T, 33-cm clear bore) equipped with a 15-cm inner diameter, actively shielded Oxford gradient coil (18 G/cm, 200- μ s rise time). The magnet, gradient coil, and Techron gradient power supply were interfaced with a Varian UNITY-INOVA console controlled by a Sun Microsystems Ultra-60 Sparc workstation. Core temperature was maintained at 37°C with circulating warm water. Coronal scout images were acquired to identify the vertebral segments using the ilium as a reference. Six transverse slices were collected covering segments T13 - L2 using a Stejskal-Tanner spin-echo diffusion weighted sequence (14) with the following acquisition parameters: TR \geq 1500 ms (determined by respiratory rate), TE = 49 ms, NEX = 4, slice thickness = 1.0 mm, FOV = 1 cm², data matrix = 128 \times 128 (zero filled to 256 \times 256). Diffusion weighted images were collected utilizing respiratory gating, and diffusion sensitizing gradients were applied in six orientations: $(G_x, G_y, G_z) = (1, 1, 0), (1, 0, 1), (0, 1, 1), (-1, 1, 0), (0, -1, 1),$ and $(1, 0, -1)$ with a gradient strength = 11.25 G/cm, duration (δ) = 10 ms, and separation (Δ) = 25 ms, to obtain a b-value of 0.785 ms/ μ m². Acquisition time was approximately two hours. DTI parameter maps were calculated for $\lambda_{||}$, λ_{\perp} , and relative anisotropy (RA) as previously described (7,9).

Histological Analysis

Immediately following imaging, spinal cords were perfusion fixed with 0.01M phosphate buffered saline (PBS) followed by 4% paraformaldehyde in PBS. Vertebral columns were excised, fixed overnight, and decalcified for 48 hours. Fixed spinal cords were embedded in paraffin and cut on a sliding microtome at a thickness of 3 μ m. The vertebral segments were used as a reference to ensure that the histological sections were from the DTI slice of interest. Sections were deparaffinized and rehydrated, and antigen retrieval was performed with sections in 1mM EDTA at 95-100°C water bath. Sections were then blocked in 2% blocking buffer (Invitrogen, Carlsbad, CA) for one hour at room temperature and incubated with polyclonal anti-myelin basic protein (1:1000, Sigma Chemical Company, St. Louis, MO) or monoclonal anti-dephosphorylated neurofilament H (SMI32, 1: 5000, Sternberger Monoclonals, Inc., Lutherville, MD) at 4°C overnight. Following rinse, goat anti-mouse or rabbit IgG conjugated with Cy3 (1:300, Jackson ImmunoResearch Laboratories, Inc., West Grove, PA) were applied to visualize immunoreactive materials. After washing, sections were covered in VECTASHIELD Mounting Medium with DAPI (Vector Laboratories, CA). Digital images were acquired on a fluorescence microscope (Nikon USA). Sections stained with the same primary antibody were acquired using identical settings for fluorescence light intensity and exposure time. The digital images utilize identical intensity scales.

Axonal damage was quantified as the number of axons per unit area that were stained positive for SMI32. Axons were manually counted on four images acquired at 20 \times magnification from

the ventral and lateral white matter from both the left and right sides of the cord. Demyelination was quantified as the percent of white matter area that exhibited abnormal or an absence of myelin basic protein (MBP) staining. Histological quantification was performed on all 10 of the active immunized EAE mice and 3 of the 5 control mice.

Statistical Analysis

Regions of interest encompassing the ventrolateral white matter were manually drawn on the DTI parameter maps using ImageJ software (15). The boundary between white matter and CSF was identified on the ADC maps, and the boundary between white matter and gray matter was identified on the RA maps. The mean white matter axial diffusivity, radial diffusivity, RA, and T2-weighted (b=0) signal-to-noise ratio (SNR) was calculated for each mouse at each imaging time point. Statistical analysis was performed for the longitudinal data (n = 6) using a repeated-measures ANOVA with an overall statistical significance of $p < 0.01$ and post-hoc tests comparing baseline with each subsequent timepoint a significance level of $p < 0.05$ with a Bonferroni correction for multiple comparisons. In the cross-sectional analysis (n = 15), correlations that included EAE Score (a discrete scale) were performed with a Spearman's rank coefficient. All other correlations utilized continuous scales and were performed with a Pearson's correlation coefficient. Both tests were considered to be significant at $p < 0.05$. Mice were also subsequently grouped according to EAE score, and groups with sufficient numbers of mice were tested for significant differences in DTI parameters between each other and between control mice using a one-way ANOVA at a significance level of $p < 0.01$ and one-way post-hoc tests at a significance level of $p < 0.05$. All statistical analysis were performed with SPSS version 15 (SPSS Inc, Chicago, IL).

Results

Longitudinal DTI of EAE

Mice with adoptive transfer EAE underwent DTI of the lumbar spinal cord at six time points following induction of the disease based on the clinical scores. The disease course was similar for all 6 mice (Fig. 1a). A decrease in axial diffusivity coincided with neurological impairment can be seen in the images from an individual mouse (Fig. 2) and in the group averaged values (Fig. 3a). Axial diffusivity was significantly different across time ($F = 27.7$, $p < 0.001$), with post-hoc test revealing significant decreases on the day of onset, the end of the acute phase, and the chronic phase compared to baseline (all $p < 0.001$). Radial diffusivity changes from baseline are demonstrated in an individual animal (Fig. 2) and showed a significant effect across time ($F = 7.3$, $p = 0.002$) in the group-averaged results (Fig. 3b). Post-hoc tests revealed that compared to baseline, radial diffusivity was increased at the end of the acute phase ($p = 0.036$) and the chronic phase ($p = 0.001$). RA decreased at the onset of clinical signs, showing an apparent decrease in an individual animal (Fig. 2) as well as significant effects across time ($F = 38.5$, $p < 0.001$) in the group-averaged results (Fig. 3c). Post-hoc test revealed that the decrease in RA compared to baseline was significant at the day of onset, end of acute, and chronic timepoints (all $p < 0.001$). T2-weighted SNR from white matter (Fig. 3d) was not significant across time ($F = 3.3$, $p < 0.023$).

DTI Correlation with Clinical Score

A cohort of mice (n = 10) with different degrees of neurological disability as assessed by EAE clinical scoring (Fig. 1b) underwent *in vivo* DTI in the chronic phase of the disease (mean clinical score at time of imaging = 2.9, s.d. = 0.99). Maps of axial diffusivity from mice reveal the decrease in axial diffusivity with the increased degree of neurological impairment (Fig. 4). There was a strong negative correlation between axial diffusivity of white matter and EAE score (Fig. 5a). Mice with EAE were subsequently grouped according to clinical score on the day of imaging. The mice with clinical scores of 2 and 4 had sufficient numbers to perform

group comparisons between each other and with control mice. Axial diffusivity had a significant effect across disease status ($F = 13.4$, $p < 0.001$). Mice with clinical scores of 2 had a significant decrease in axial diffusivity compared with the control mice ($p = 0.030$), as did mice with clinical scores of 4 ($p < 0.001$). Furthermore, mice with clinical scores of 4 also had a significant decrease in axial diffusivity compared to mice with clinical scores of 2 ($p = 0.037$). Histological sections stained for axonal damage using SMI-32 demonstrate an overall increase in positively stained axons in mice with severe EAE compared with those with moderate EAE (Figs. 6 a-c). There was a significant correlation between EAE clinical score and the number of axons staining positive for SMI-32 (Fig. 7a). The number of injured axons had a significant effect across disease status ($F = 15.3$, $p = 0.001$), and was significantly different between control mice and mice with clinical scores of 4 ($p < 0.001$), and between mice with clinical scores of 2 and those with clinical scores of 4 ($p = 0.002$). Furthermore, the number of injured axons had a significant negative correlation with axial diffusivity (Fig. 7c).

Radial diffusivity increased in the spinal cord white matter of mice with EAE compared to controls (Fig. 4). Radial diffusivity had a weak, but significant, correlation with EAE clinical score (Fig. 5b). There was a significant effect of EAE clinical score on radial diffusivity ($F=18.8$, $p < 0.001$). Compared to control mice, radial diffusivity significantly increased in mice with a clinical score of 2 ($p < 0.001$) and mice with a clinical score of 4 ($p = 0.003$). However, the radial diffusivity between mice with a clinical score of 2 and those with a clinical score of 4 was not significantly different ($p = 0.19$). Histological sections stained for MBP demonstrated a decrease in staining intensity in mice with EAE compared to controls (Fig. 6 d-f), as well as a loss of myelin integrity apparent at high magnification. The percent of demyelinated white matter area was significantly correlated with EAE score (Fig. 7b), but did not have a significant effect across EAE scores ($F = 5.6$, $p = 0.021$). The percent of demyelinated area did not significantly correlate with radial diffusivity (Fig. 7d).

RA maps (Fig. 4) also demonstrate an obvious decrease in RA in mice with EAE compared to control white matter. RA had a strong negative correlation with EAE clinical score (Fig. 5c), but RA did not scale with EAE severity. An overall effect of clinical score on RA was significant ($F = 43.5$, $p < 0.001$). Compared to control mice, RA decreased in mice with a clinical score of 2 ($p < 0.001$) and mice with a clinical score of 4 ($p < 0.001$). However, RA in mice with clinical scores of 2 and in those with clinical scores of 4 was nearly identical. T2-weighted SNR was not correlated with clinical score (Fig. 5d) and did not have a significant effect across EAE score ($F = 0.3$, $p = 0.718$).

None of the DTI parameters from dorsal white matter correlated with EAE scores (data not shown).

Discussion

An increasing body of evidence from animal studies has shown that axial and radial diffusivities derived from DTI hold promise as biomarkers of axonal damage and demyelination, respectively (7-9,16,17). A decrease in axial diffusivity has been shown to be indicative of axonal damage in EAE (13,18), whereas an increase in radial diffusivity has been shown to be a noninvasive marker of demyelination or dysmyelination. In the current study, *in vivo* DTI of the murine spinal cord was used to investigate the relationship between the directional diffusivities and clinical impairment.

The adoptive transfer EAE model leads to a predictable and well-characterized time course (Fig. 1a) of acute impairment attributable to inflammation, followed by chronic impairment attributable to axonal damage (19). In the current study, mice with adoptive transfer EAE underwent longitudinal DTI measurements. A decrease in axial diffusivity coincided with the

onset of clinical signs and persisted into the chronic phase, whereas radial diffusivity was significantly different from baseline only in the later stages (Fig. 3). Thus, it was hypothesized that axial diffusivity is the primary correlate of clinical impairment in EAE.

Mice with EAE induced through active immunization display a greater heterogeneity of neurological impairment compared to the adoptive transfer model (Fig. 1b). The degree of axonal damage in chronic EAE has been shown to be the primary correlate of clinical scores in chronic EAE (20,21). Mice with chronic EAE induced through active immunization underwent *in vivo* DTI in order to determine whether axial or radial diffusivity correlated with neurological disability. As hypothesized, axial diffusivity significantly correlated with EAE score (Fig. 5a). Furthermore, decreases in axial diffusivity were associated with more severe axonal damage (Fig. 6). The number of injured axons highly correlated with both EAE score and axial diffusivity (Fig. 7). In contrast, radial diffusivity did not correlate with disability, and the area of demyelinated white matter did not correlate with either EAE score or radial diffusivity. RA was sensitive in differentiating mice with EAE from those without the disease, but did not scale with increasing impairment. Axial diffusivity was a better indicator of the degree of neurological disability than either RA or radial diffusivity.

Overall, these experiments demonstrate that axial diffusivity correlated with neurological impairment and axonal damage in EAE. Changes in axial diffusivity could be an important parameter linking axonal dysfunction and outward clinical impairment in CNS white matter disorders. Axial diffusivity may be especially sensitive to pathology since injury to an axon is likely to affect all levels distal to the injury. In contrast, demyelination can be more focal and may span only a small portion of a single DTI slice. Further experiments are necessary, in both animals and humans, to establish the utility and reliability of the directional diffusivities as markers of damage in the CNS. Elucidating the early structural and metabolic events in EAE and MS that cause the changes in diffusivities will add to the specificity of DTI as a noninvasive marker of pathology.

Establishing a link between MRI and disability in MS has so far proven difficult. Many different MRI parameters have been investigated, including brain atrophy (22-24), lesion location (25), lesion load (26), magnetization transfer ratio (27), or a composite of several methods (28). These imaging parameters have had only modest correlations with the most widely used MS clinical assessments, the Kurtzke Expanded Disability Status Score (EDSS) or the Multiple Sclerosis Functional Composite (MSFC). Although axonal integrity measured with magnetic resonance spectroscopy (MRS) has had some success in correlating with disability, reports have been conflicting (29-31).

Spinal cord lesions are a common finding in MS, being found in the majority of MS patients (32). Lesions to the cord significantly impair motor functions. Not surprisingly, spinal cord atrophy and *ex vivo* DTI of the cord have shown some of the strongest correlations with impairment (33,34). Less work has focused on DTI of the human spinal cord *in vivo*, possibly due to technical challenges caused by the bone/tissue interfaces and motion related artifacts (16). However, its coherent arrangement of axonal fibers has potential for very accurate measurements of axial and radial diffusivities. Future studies will determine whether the ability of DTI to discriminate pathology in the spinal cord of animal models will carry over to the human situation. If it does, the link could prove beneficial in the clinical management of MS and as an outcome measure in clinical trials. The relationship between neurological disability and axial diffusivity of the mouse spinal cord presented herein represents a critical step closer to a noninvasive biomarker of axonal injury in MS.

Acknowledgements

The authors thank the following sources for funding support: National Multiple Sclerosis Society (RG 3376-A-2/1, and CA 1012-A-13), NIH (R01-NS054194), and the Washington University Small Animal Imaging Resource (WUSAIR) (NIH: R24-CA83060). M.D.B. is supported by a NIH/NINDS predoctoral fellowship (F31-NS052057). J.H.K. is supported by a grant from the University of Missouri Spinal Cord Injuries Research Program (06-6401).

References

1. McDonald WI, Compston A, Edan G, Goodkin D, Hartung HP, Lublin FD, McFarland HF, Paty DW, Polman CH, Reingold SC, Sandberg-Wollheim M, Sibley W, Thompson A, van den Noort S, Weinshenker BY, Wolinsky JS. Recommended diagnostic criteria for multiple sclerosis: guidelines from the International Panel on the diagnosis of multiple sclerosis. *Ann Neurol* 2001;50(1):121–127. [PubMed: 11456302]
2. Barkhof F. The clinico-radiological paradox in multiple sclerosis revisited. *Curr Opin Neurol* 2002;15(3):239–245. [PubMed: 12045719]
3. Barkhof F. MRI in multiple sclerosis: correlation with expanded disability status scale (EDSS). *Mult Scler* 1999;5(4):283–286. [PubMed: 10467389]
4. McFarland HF, Barkhof F, Antel J, Miller DH. The role of MRI as a surrogate outcome measure in multiple sclerosis. *Mult Scler* 2002;8(1):40–51. [PubMed: 11936488]
5. Schwartz ED, Chin CL, Shumsky JS, Jawad AF, Brown BK, Wehrli S, Tessler A, Murray M, Hackney DB. Apparent diffusion coefficients in spinal cord transplants and surrounding white matter correlate with degree of axonal dieback after injury in rats. *AJNR Am J Neuroradiol* 2005;26(1):7–18. [PubMed: 15661691]
6. Schwartz ED, Cooper ET, Fan Y, Jawad AF, Chin CL, Nissanov J, Hackney DB. MRI diffusion coefficients in spinal cord correlate with axon morphometry. *Neuroreport* 2005;16(1):73–76. [PubMed: 15618894]
7. Song SK, Sun SW, Ramsbottom MJ, Chang C, Russell J, Cross AH. Demyelination revealed through MRI as increased radial (but unchanged axial) diffusion of water. *Neuroimage* 2002;17(3):1429–1436. [PubMed: 12414282]
8. Sun SW, Liang HF, Trinkaus K, Cross AH, Armstrong RC, Song SK. Noninvasive detection of cuprizone induced axonal damage and demyelination in the mouse corpus callosum. *Magn Reson Med* 2006;55(2):302–308. [PubMed: 16408263]
9. Song SK, Sun SW, Ju WK, Lin SJ, Cross AH, Neufeld AH. Diffusion tensor imaging detects and differentiates axon and myelin degeneration in mouse optic nerve after retinal ischemia. *Neuroimage* 2003;20(3):1714–1722. [PubMed: 14642481]
10. Sabelko-Downes KA, Cross AH, Russell JH. Dual role for Fas ligand in the initiation of and recovery from experimental allergic encephalomyelitis. *J Exp Med* 1999;189(8):1195–1205. [PubMed: 10209037]
11. Okuda Y, Okuda M, Bernard CC. Gender does not influence the susceptibility of C57BL/6 mice to develop chronic experimental autoimmune encephalomyelitis induced by myelin oligodendrocyte glycoprotein. *Immunol Lett* 2002;81(1):25–29. [PubMed: 11841842]
12. Cross AH, Misko TP, Lin RF, Hickey WF, Trotter JL, Tilton RG. Aminoguanidine, an inhibitor of inducible nitric oxide synthase, ameliorates experimental autoimmune encephalomyelitis in SJL mice. *J Clin Invest* 1994;93(6):2684–2690. [PubMed: 7515395]
13. Kim JH, Budde MD, Liang HF, Klein RS, Russell JH, Cross AH, Song SK. Detecting axon damage in spinal cord from a mouse model of multiple sclerosis. *Neurobiol Dis* 2006;21(3):626–632. [PubMed: 16298135]
14. Stejskal EO, Tanner JE. Spin Diffusion Measurements: Spin Echoes in the Presence of a Time-Dependent Field Gradient. *J Chem Phys* 1965;42(1):288–292.
15. Rasband, WS. ImageJ. U. S. National Institutes of Health; Bethesda, Maryland, USA: 19972005.
16. Wheeler-Kingshott CA, Hickman SJ, Parker GJ, Ciccarelli O, Symms MR, Miller DH, Barker GJ. Investigating cervical spinal cord structure using axial diffusion tensor imaging. *Neuroimage* 2002;16(1):93–102. [PubMed: 11969321]

17. Nair G, Tanahashi Y, Low HP, Billings-Gagliardi S, Schwartz WJ, Duong TQ. Myelination and long diffusion times alter diffusion-tensor-imaging contrast in myelin-deficient shiverer mice. *Neuroimage* 2005;28(1):165–174. [PubMed: 16023870]
18. Budde MD, Kim JH, Liang HF, Schmidt RE, Russell JH, Cross AH, Song SK. Toward accurate diagnosis of white matter pathology using diffusion tensor imaging. *Magn Reson Med* 2007;57(4):688–695. [PubMed: 17390365]
19. Rao P, Segal BM. Experimental autoimmune encephalomyelitis. *Methods Mol Med* 2004;102:363–375. [PubMed: 15286395]
20. Wujek JR, Bjartmar C, Richer E, Ransohoff RM, Yu M, Tuohy VK, Trapp BD. Axon loss in the spinal cord determines permanent neurological disability in an animal model of multiple sclerosis. *J Neuropathol Exp Neurol* 2002;61(1):23–32. [PubMed: 11829341]
21. Papadopoulos D, Pham-Dinh D, Reynolds R. Axon loss is responsible for chronic neurological deficit following inflammatory demyelination in the rat. *Exp Neurol* 2006;197(2):373–385. [PubMed: 16337942]
22. Kalkers NF, Bergers E, Castelijns JA, van Walderveen MA, Bot JC, Ader HJ, Polman CH, Barkhof F. Optimizing the association between disability and biological markers in MS. *Neurology* 2001;57(7):1253–1258. [PubMed: 11591845]
23. Benedict RH, Weinstock-Guttman B, Fishman I, Sharma J, Tjoa CW, Bakshi R. Prediction of neuropsychological impairment in multiple sclerosis: comparison of conventional magnetic resonance imaging measures of atrophy and lesion burden. *Arch Neurol* 2004;61(2):226–230. [PubMed: 14967771]
24. Tjoa CW, Benedict RH, Weinstock-Guttman B, Fabiano AJ, Bakshi R. MRI T2 hypointensity of the dentate nucleus is related to ambulatory impairment in multiple sclerosis. *J Neurol Sci* 2005;234(12):17–24. [PubMed: 15993137]
25. Charil A, Zijdenbos AP, Taylor J, Boelman C, Worsley KJ, Evans AC, Dagher A. Statistical mapping analysis of lesion location and neurological disability in multiple sclerosis: application to 452 patient data sets. *Neuroimage* 2003;19(3):532–544. [PubMed: 12880785]
26. Sinnige LG, Teeuwissen E, Hew JM, Minderhoud JM. Correlation between magnetic resonance imaging and clinical parameters in multiple sclerosis. *Acta Neurol Scand* 1995;91(3):188–191. [PubMed: 7793233]
27. Santos AC, Narayanan S, de Stefano N, Tartaglia MC, Francis SJ, Arnaoutelis R, Caramanos Z, Antel JP, Pike GB, Arnold DL. Magnetization transfer can predict clinical evolution in patients with multiple sclerosis. *J Neurol* 2002;249(6):662–668. [PubMed: 12111296]
28. Mainero C, De Stefano N, Iannucci G, Sormani MP, Guidi L, Federico A, Bartolozzi ML, Comi G, Filippi M. Correlates of MS disability assessed in vivo using aggregates of MR quantities. *Neurology* 2001;56(10):1331–1334. [PubMed: 11376183]
29. Narayana PA, Wolinsky JS, Rao SB, He R, Mehta M. Multicentre proton magnetic resonance spectroscopy imaging of primary progressive multiple sclerosis. *Mult Scler* 2004;10(Suppl 1):S73–78. [PubMed: 15218814]
30. Bonneville F, Moriarty DM, Li BS, Babb JS, Grossman RI, Gonen O. Whole-brain N-acetylaspartate concentration: correlation with T2-weighted lesion volume and expanded disability status scale score in cases of relapsing-remitting multiple sclerosis. *AJNR Am J Neuroradiol* 2002;23(3):371–375. [PubMed: 11901002]
31. De Stefano N, Narayanan S, Francis GS, Arnaoutelis R, Tartaglia MC, Antel JP, Matthews PM, Arnold DL. Evidence of axonal damage in the early stages of multiple sclerosis and its relevance to disability. *Arch Neurol* 2001;58(1):65–70. [PubMed: 11176938]
32. Lovas G, Szilagyi N, Majtenyi K, Palkovits M, Komoly S. Axonal changes in chronic demyelinated cervical spinal cord plaques. *Brain* 2000;123(Pt 2):308–317. [PubMed: 10648438]
33. Losseff NA, Webb SL, O’Riordan JI, Page R, Wang L, Barker GJ, Tofts PS, McDonald WI, Miller DH, Thompson AJ. Spinal cord atrophy and disability in multiple sclerosis. A new reproducible and sensitive MRI method with potential to monitor disease progression. *Brain* 1996;119(Pt 3):701–708. [PubMed: 8673483]

34. Stevenson VL, Leary SM, Losseff NA, Parker GJ, Barker GJ, Husmani Y, Miller DH, Thompson AJ. Spinal cord atrophy and disability in MS: a longitudinal study. *Neurology* 1998;51(1):234–238. [PubMed: 9674808]

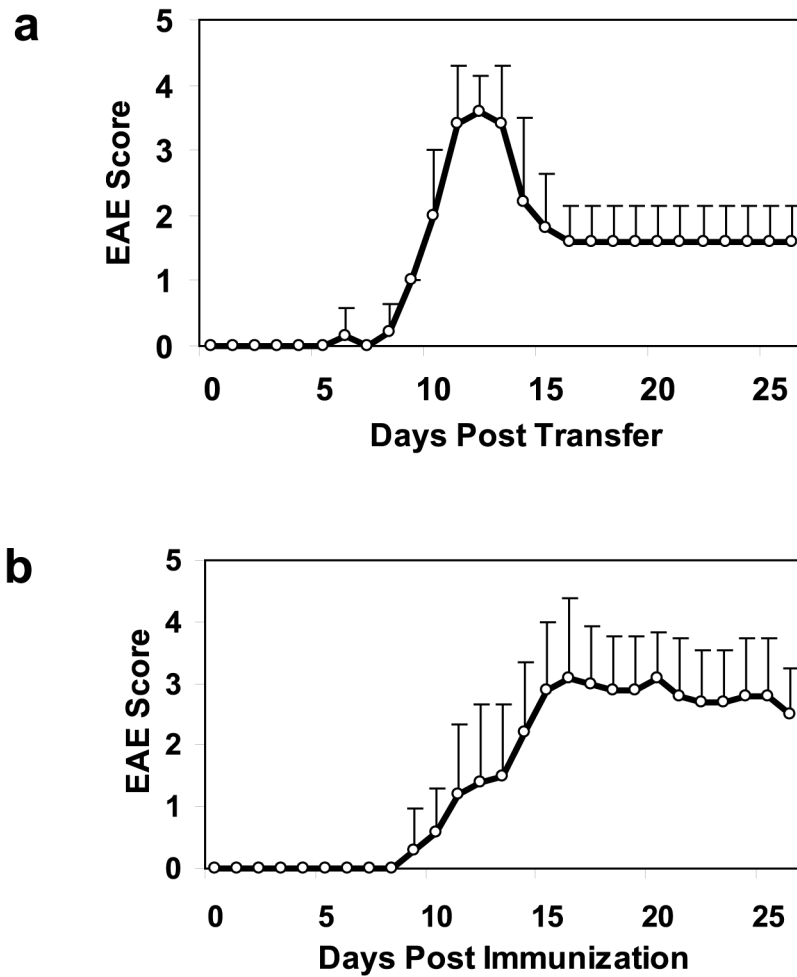


Figure 1. Clinical course for EAE induced in mice using adoptive transfer (a) and active immunization (b). Adoptive transfer EAE ($n = 6$) produces a more reproducible clinical course, whereas EAE induced through active immunization ($n = 10$) produces a greater heterogeneity in clinical course. Values are expressed as mean daily score \pm s.d.

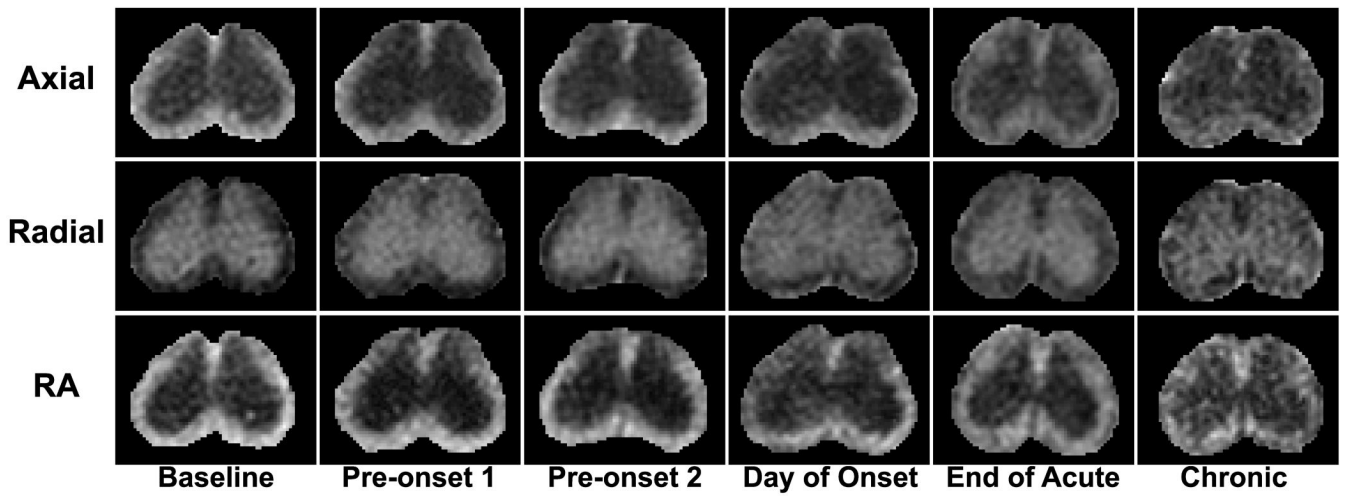


Figure 2.

The DTI parameter maps at vertebral segment L1 are shown from a single mouse imaged six times in the month following induction of EAE through adoptive transfer. A decrease in white matter axial diffusivity and RA is seen beginning at the onset of clinical signs.

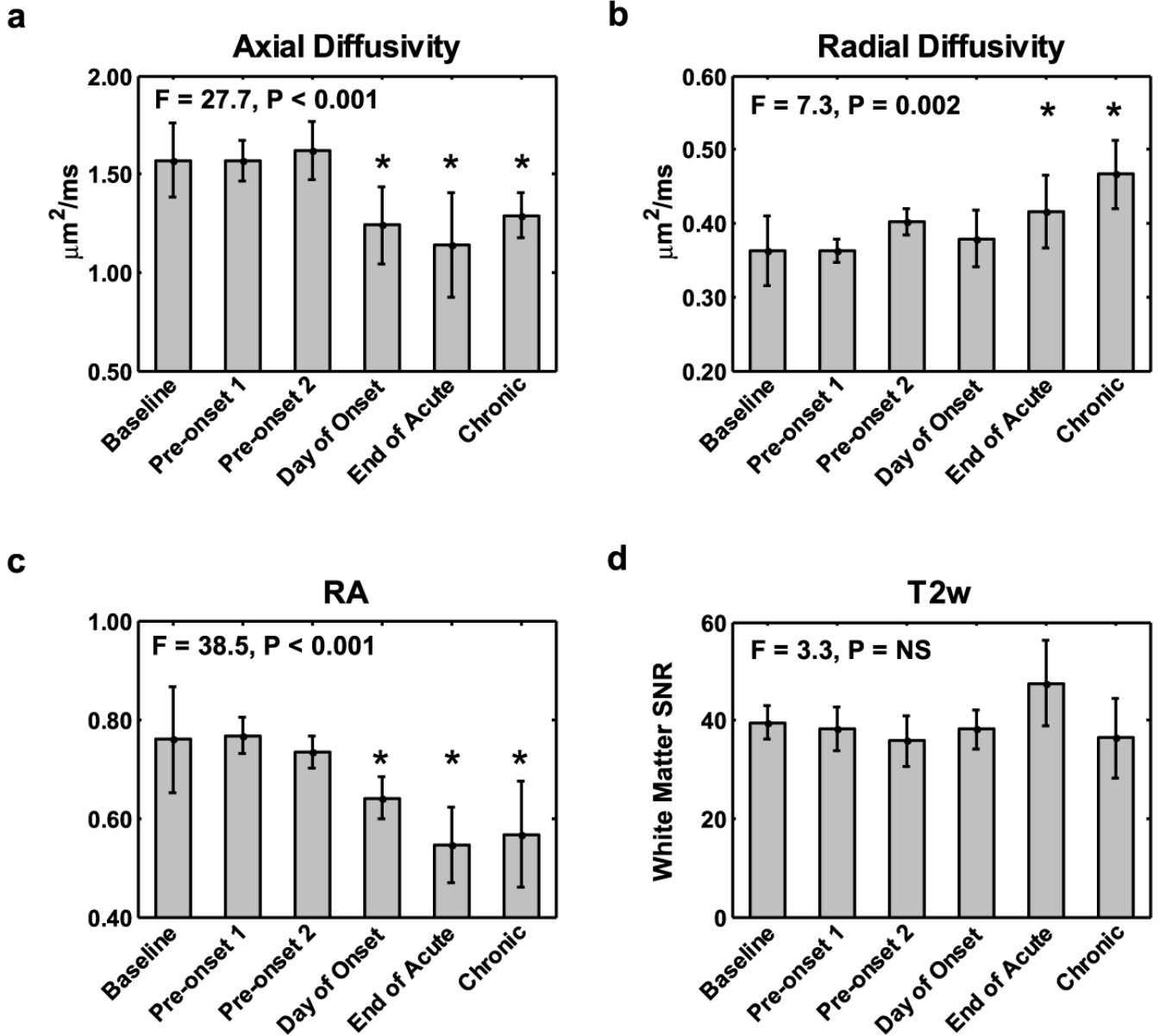


Figure 3. The group-averaged ($n = 6$) DTI parameters show a decrease in axial diffusivity (a) occurring at the onset of clinical signs that persists into the chronic phase of the disease. Radial diffusivity (b) increases early in the time course but is not significant until after the acute phase of the disease. RA (c) decreases throughout the disease course. T2-weighted SNR (d) was not significantly different at any timepoint. Values are expressed as mean \pm s.d. * = post-hoc test significantly different from baseline, $p < 0.05$.

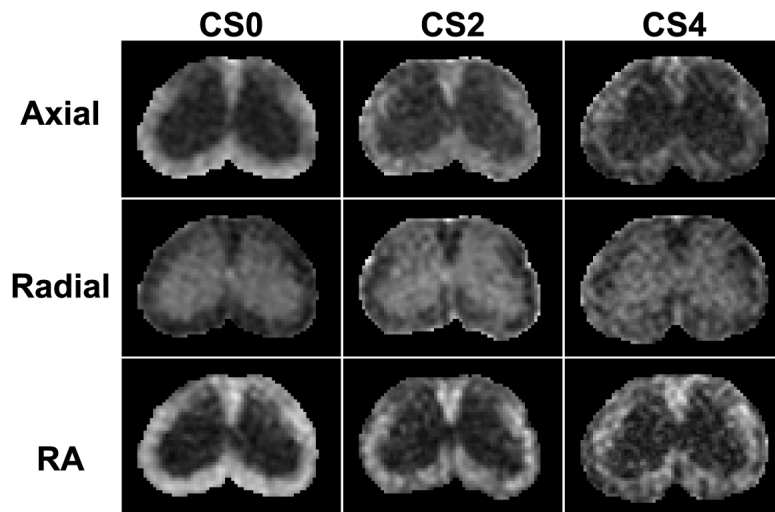


Figure 4. The DTI parameter maps from a control mouse (left), a mouse with clinical score of 2 (center), and a mouse with a clinical score of 4 (right) one month after the induction of EAE through active immunization. Increasing disease severity leads to an obvious loss of white matter integrity depicted as a decrease in both axial diffusivity and RA and an increase in radial diffusivity.

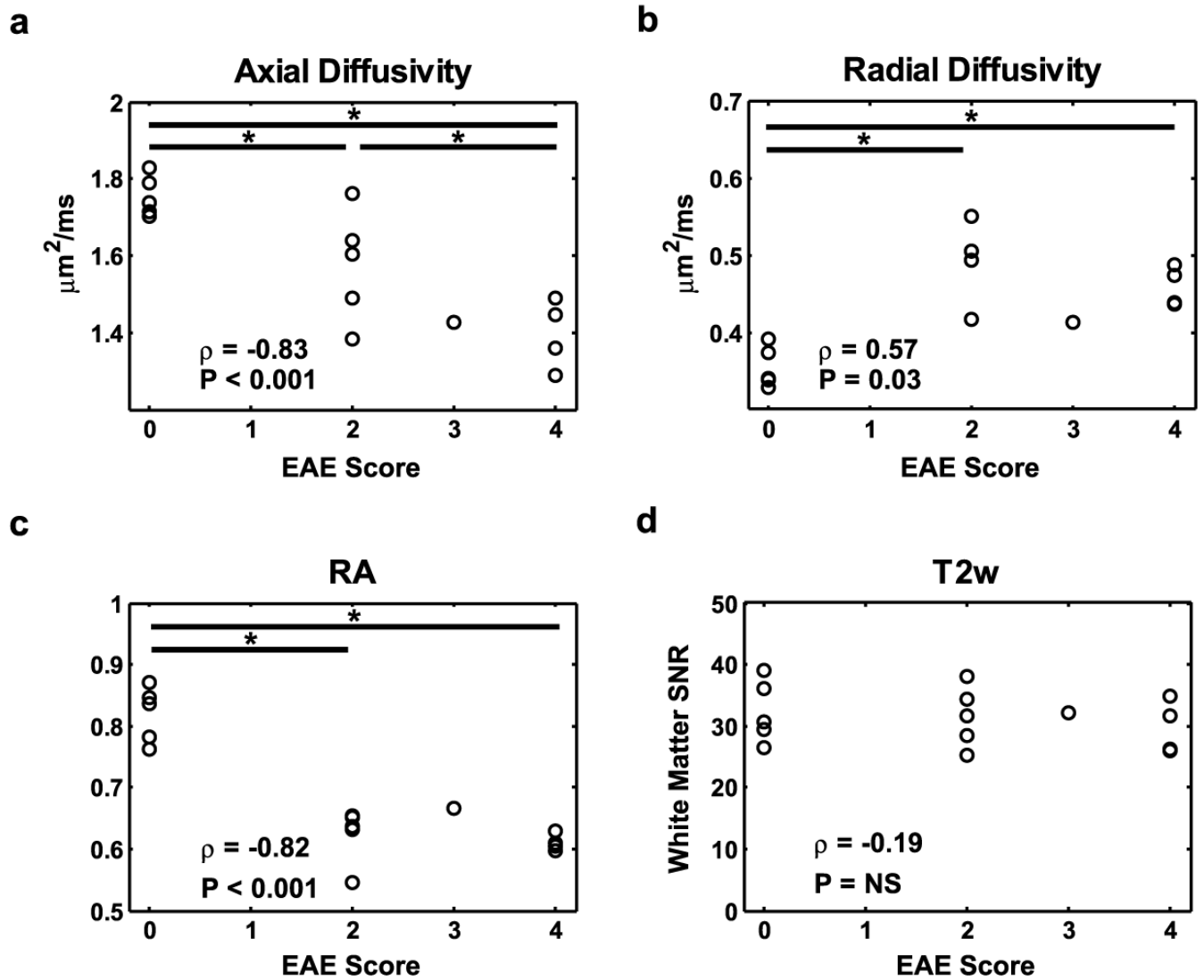


Figure 5. A Spearman's rank correlation analysis demonstrates the correlation between EAE scores and DTI parameters from ventrolateral white matter. See text for additional details. * - $p < 0.05$.

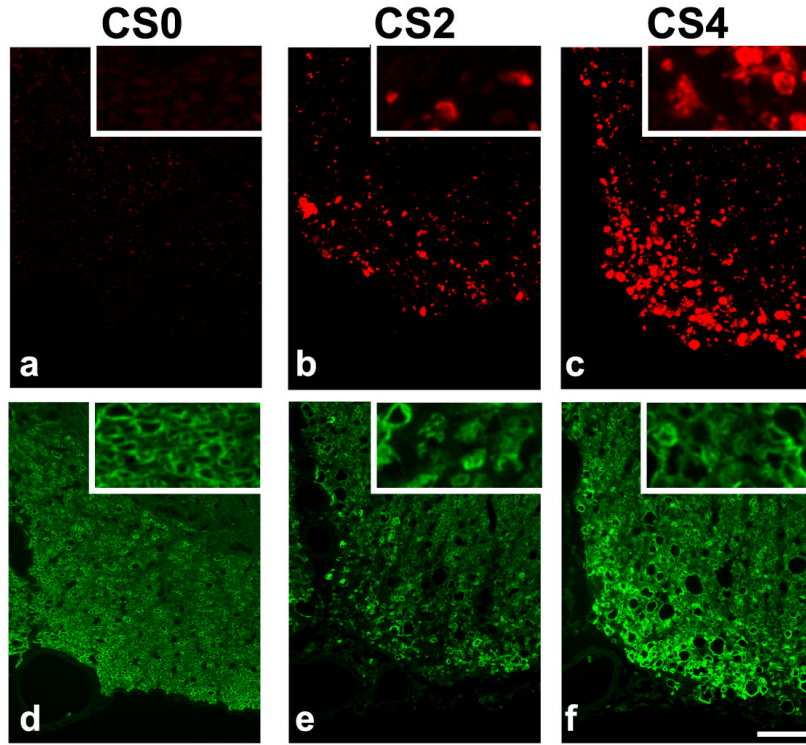


Figure 6. Spinal cord sections were stained for injured axons (SMI-32; top) and myelin (MBP, bottom). No SMI32 positive axons are seen in the ventral white matter of the control cord (a), but the number of positively stained axons increases in moderate EAE (b; clinical score = 2) and further increases in severe EAE (c; clinical score = 4). Well-defined myelin rings are seen in the MBP stain from a control cord (d). A loss of MBP staining is evidence of demyelination in mice with moderate (e) and severe (f) EAE, and the myelin rings have lost their integrity in the EAE cord (e & f, insets). Scale bar indicates 50 μ m.

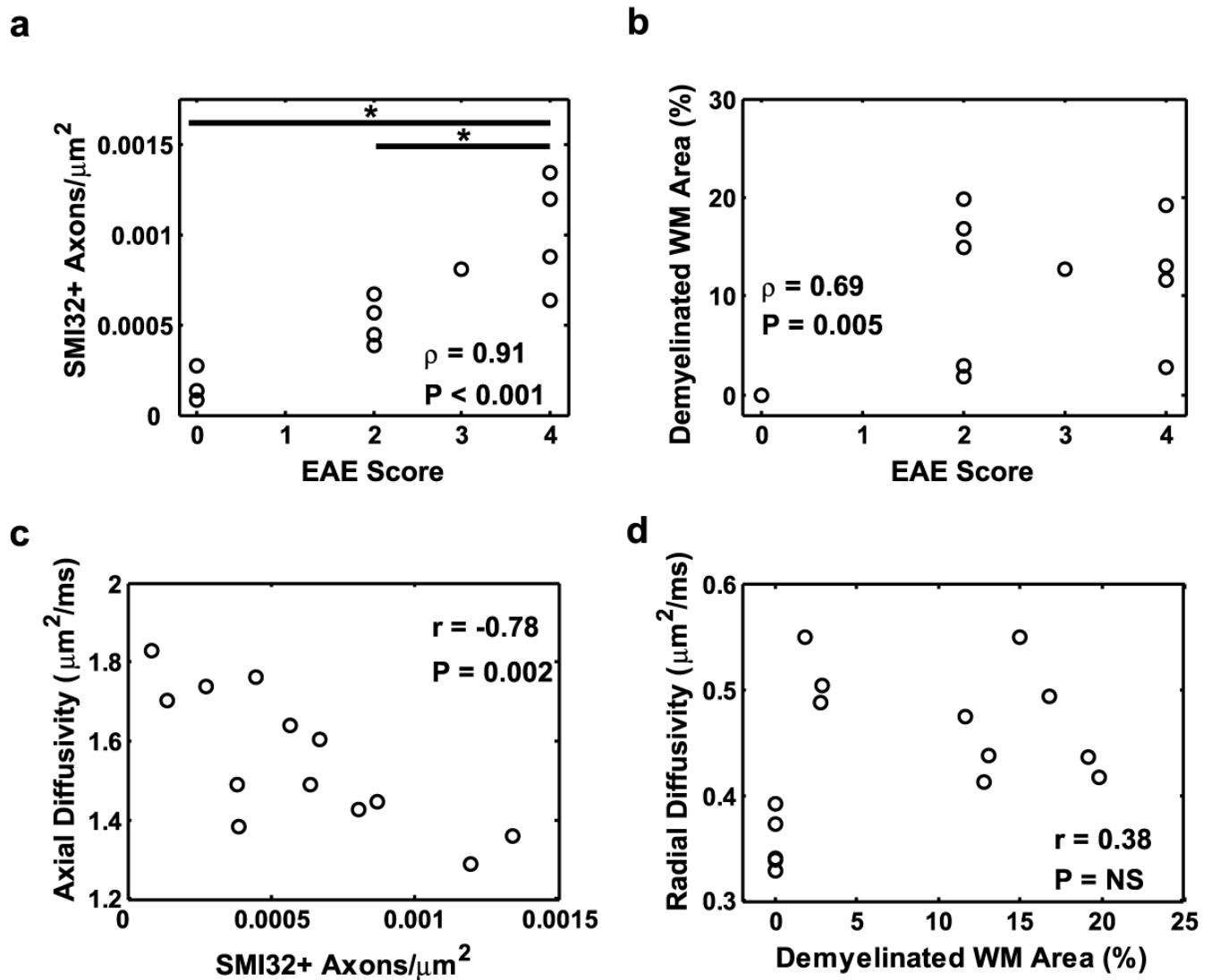


Figure 7. Correlations between quantitative histological parameters and EAE scores demonstrate a strong relationship between axonal damage and EAE score (a), with the number of damaged axons differentiating mice with moderate or severe EAE. Demyelination is moderately correlated with EAE score (b), but does not differentiate mice with different EAE scores. Axial diffusivity highly correlated with the number of injured axons (c). Radial diffusivity did not correlate with the percent of demyelinated area (d). * - $p < 0.05$.